

Design and Implementation of Dynamic Time History Analysis in Building Structure CAD

Xia Wang

Tianjin Chengjian University, Tianjin, China

wangxia@tcu.edu.cn

Keywords: Building Structure, CAD, Seismic Strengthening, Elastoplasticity, Dynamic Time History Analysis

Abstract: With the continuous development of the construction industry at home and abroad, the dynamic time history analysis has become increasingly important, and the current level of analysis of the dynamic time history is not high enough, and the importance of research cannot be ignored. In order to solve the problem that the dynamic time history analysis of the building structure is not comprehensive and not thorough enough, this paper analyzes the dynamic time history of the building structure CAD and finds that the reinforced concrete frame structure can be more effective than the pure frame structure under the horizontal static load. The lateral displacement is limited; the seismic reinforcement effects of C/GFRP and CFRP fiber materials are compared respectively, and three different schemes are analyzed and compared: reinforcement of the first layer, reinforcement of the first to third layers, and reinforcement of all layers. Under the action of El seismic wave and Taft wave, the maximum interlayer displacement angle of C/GFRP, CFRP strengthened and unreinforced frame structures were used respectively. In this paper, the dynamic time history analysis in the building structure is studied. Based on the motion balance equation of a model under earthquake action, the Newmark- β method is used to analyze the dynamic time history and design in the building structure. The results are applied to the design of building structures to optimize the performance of building structures, and also provide a basis for the development and improvement of seismic design calculation methods for building structures.

1. Introduction

The development of architectural CAD technology has been divided into two stages in terms of its technical components and auxiliary functions: First, the first generation of CAD technology, mainly using computers for auxiliary calculation and analysis. In the early days of CAD

development, due to the limitations of hardware and basic software, there was no graphical interaction, and the computer only assisted the designer in completing complex analytical calculations; Second, the second generation CAD system. The series of products of large software development companies such as building structure CAD system occupy the main market of the domestic architectural design industry. These series of software not only can meet the design structure design of the design institute, but also the version is changing with each passing day, the function is getting better and better, and the work efficiency is continuously improved. So far, the engineering design industry is one of the more mature industries in China.

For the CAD technology of building structure, many research teams at home and abroad have already conducted in-depth research. Vikram A [1] reviewed the current trends in lithography and related resolution enhancement techniques, and briefly introduced the integrated CAD analysis of hotspot detection. Yu R [2] proposed a performance-based anti-explosion design method. Emphasizes some key issues in the design process and presents general design ideas and procedures. Brouwer D H [3] proposed the use of this NMR crystallographic method to determine the structure of a surfactant-templated layered silicate material that lacks complete three-dimensional crystallinity. Hartmann André [4] describes a new data integration workflow that quantifies the structure and dynamics of national buildings by analyzing authoritative geographic data. Russo D [5] combines the principles of ecological innovation with design methods based on structural optimization tools to create a knowledgeable CAE process that links CAD, FEM, optimization tools and LCA-based tools. Wei G [6] characterized the chemical structure and morphology of the composite by Fourier transform infrared spectroscopy, thermogravimetric analysis and transmission electron microscopy. Li L [7] proposed a closed-loop recognition algorithm (CLR), multi-closed-loop intelligent identification (MCLR) algorithm and multi-closed-loop matching (MCLM) algorithm based on feature recognition, which realized the automatic generation of regular surfaces in the flow channel. With the rapid development of modern computer technology, CAD technology has been widely used in various industries [8]. Ren Zhenyu [9] introduced the characteristics of high-rise buildings, expounded the design principles of high-rise building structures, and analyzed the application value of CAD technology in high-rise building structure design. Yan Shuaiping [10] analyzed the main problems existing in the seismic design of building engineering structures, and proposed an effective design strategy for improving the seismic capacity of building engineering structures. Yao Xianchun [11] designed the blasting parameters of columns, shear walls and beams respectively, and adopted the optimized blasting network and safety protection measures to ensure the smooth implementation of blasting demolition.

At present, the computer-aided design technology of various industries in China has developed rapidly, and the CAD system involving various structures has been basically improved. However, the development of CAD systems for some special structures (such as multi-level, high-rise complex building structures, etc.) lags far behind the general application software. The dynamic time history analysis method overcomes this limitation of the response spectrum direction. Users can input seismic waves based on the results of geological surveys and historical seismic records in the area. Different seismic waves will have different effects and damage to the same building.

Due to the unique advantages of dynamic time history analysis, domestic and foreign research teams apply dynamic time history analysis in various fields. Liu S W [12] proposed the dynamic time-history elastic analysis of each unit model in the field of mechanical calculation. The curved arbitrary positioning hinge (ALH) beam-column unit was used directly to integrate the Newmark algorithm. Samuel B [13] applied dynamic time history analysis to quality evaluation and designed a simple optical configuration for developing dynamic speckle image systems to record dynamic speckle patterns of samples under different conditions. Choine M N [14] applied dynamic time history analysis to performance evaluation, and used a new corrosion reinforced constitutive model

to investigate the effect of steel corrosion in reinforced concrete columns on the seismic performance of multi-span concrete bridges. Tong Z [15] applied the dynamic time history analysis to the model test. Based on the centrifugal model test platform, the dynamic model test was carried out to study the law of anchoring pile reinforcement landslide under the condition of 50 g centrifugal acceleration. Li S [16] evaluated the accuracy and applicability of POA by comparison with dynamic time history analysis (THA). The dynamic time history analysis was verified by the ductile RC frame complete collapse shaking table test. Koo R C H [17] applied dynamic time history analysis to stability analysis, and used the representative time history of bedrock blasting vibration from actual on-site monitoring data and numerical site response analysis to evaluate the dynamic stability of soil slope.

In order to solve the problem that the dynamic time history analysis of the building structure is not comprehensive and not thorough enough, this paper analyzes the dynamic time history of the building structure CAD. Under the horizontal static load, the reinforced concrete analysis frame structure can be more effective than the pure frame structure. Limit lateral displacement; Accurate and comprehensive analysis of the structure from the internal forces, deformations and structural members in the linear and non-linear stage structure gradually cracking, yielding, breaking to final collapse; using C/GFRP and CFRP fibers respectively The seismic strengthening effects of the materials were compared, and three different schemes were analyzed and compared: only the first layer was reinforced, the first layer to the third layer were reinforced, and the reinforcement effect of all layers was strengthened. Under the action of El seismic wave and Taft wave, the maximum interlayer displacement angle of C/GFRP, CFRP strengthened and unreinforced frame structures were used respectively.

2. Method

2.1. Application of Newmark- β Algorithm in Dynamic Time History Analysis

Assuming that the displacement, velocity, and acceleration at time t have been found, it is now required to resolve the reaction at time $t+\Delta t$. That is, to satisfy the equation:

$$M\ddot{X}_{t+\Delta t}(t) + C\dot{X}_{t+\Delta t}(t) + KX_{t+\Delta t}(t) = -M\ddot{Z}(t)_{t+\Delta t}$$

The Newmark- β method introduces the following acceleration, velocity, and displacement relationships:

$$\begin{aligned} X_{t+\Delta t} &= X_t + \dot{X}_t\Delta t + (1/2 - \beta)\ddot{X}_t\Delta t^2 + \beta\ddot{X}_{t+\Delta t}\Delta t^2 \\ \dot{X}_{t+\Delta t} &= \dot{X}_t + (1 - \gamma)\ddot{X}_t\Delta t + \gamma\ddot{X}_{t+\Delta t}\Delta t \\ \ddot{X}_{t+\Delta t} &= \frac{1}{\beta\Delta t^2}(X_{t+\Delta t} - X_t) - \frac{1}{\beta\Delta t}\dot{X}_t - \left(\frac{1}{2\beta} - 1\right)\ddot{X}_t \end{aligned}$$

$\ddot{Z}_{t+\Delta t}$: the acceleration of the ground motion at the time $t+\Delta t$;

$X_t, X_{t+\Delta t}, \Delta X_{t+\Delta t}$: displacement of the structure at time t , displacement and displacement increment in the $t+\Delta t$ time interval, respectively.

The principle of this method is to retain the acceleration term by the expansion of the Taylor series, introducing two parameters γ and β as corrections for the truncated high-order small quantities. Newmark- β indicates that $\gamma < 0.5$ will produce negative damping, which leads to an increase in amplitude in the integral calculation; when $\gamma > 0.5$ will produce artificial damping, so that the amplitude is artificially attenuated, $\gamma > 0.5$ is generally used. The most common is to take $\gamma = 0.5$, and then change β , β changes to indicate the different selection of acceleration in the integration process.

When we know the displacement, velocity and acceleration at time t , we can establish the equation about the displacement $X_{t+\Delta t}$ at $t+\Delta t$. Solving the equation can obtain the displacement at $t+\Delta t$. It can be seen from the above equation that in the implicit integral, except that the stiffness matrix and the node force vector contain the difference between the inertia and the damping of the system, the equations of the dynamic nonlinear analysis have the same equations as the static nonlinear analysis. Form, therefore, the solution to the nonlinear equation discussed in the static analysis can be used to solve the dynamic nonlinear equation.

2.2. Nonlinear Analysis Unit Model

(1) Skeleton line

The α - ε relationship of the steel bars is:

$$\sigma = \begin{cases} E_s \varepsilon, & \varepsilon \leq \varepsilon_y \\ f_y, & \varepsilon_y \leq \varepsilon \leq \varepsilon_{yu} \\ f_y + 0.01(\varepsilon - \varepsilon_{yu}), & \varepsilon > \varepsilon_{yu} \end{cases}$$

E_s -reinforcing elastic modulus; ε -steel strain; ε_y -steel yield strain; α -reinforced steel stress;

f_y -reinforced steel yield strength; ε_{yu} - corresponds to the strain of the end of the steel plate α - ε curve yielding platform, this paper takes 0.02.

If the section is divided into meshes, the program will have good versatility, and it can calculate any section and oblique force. It is only necessary to form specific section information for different sections. The specific method is to fill any section. It is divided into rectangles, which are divided into grids. Each grid is distinguished by the corresponding information according to its material, whether it is a blank grid, and whether the strain is maximum. In order to facilitate the programming, we stipulate that the compressive strain of the section is taken as a negative value, and the tensile strain is taken as positive: the bending moment, the curvature is positive in the clockwise direction, and the counterclockwise direction is negative. The reference axis x -axis is placed on the centerline of the section and perpendicular to the moment-applying plane: the y -axis passes through the center of the section and is perpendicular to the x -axis.

(2) Section bending moment-curvature relationship, feature point calculation

1) reading the basic information of the component;

2) taking the initial curvature Φ , the initial strain of the intermediate section is 0, the initial curvature increment $\delta\varphi = 5 \times 10^{-5}$, and the initial strain increment $\delta\varepsilon = 5 \times 10^{-5}$;

3) Calculate the strain ε of each strip and the stress of steel and concrete, find the sum of internal force N and internal moment of each strip, record the crack of concrete, the yield of steel, the curvature and bending moment of concrete crushing, and check whether it is satisfied. Balance condition of the section;

4) If the equilibrium condition is not satisfied, $\bar{\varepsilon} = \bar{\varepsilon} + \delta\varepsilon$, after the corresponding internal

$$\bar{\varepsilon} = \bar{\varepsilon} + \delta\varepsilon \cdot \frac{N - N_2}{N_2 - N_1}$$

force N_2 is obtained, an interpolation method is used to obtain a new on the axial stress N of the member.

5) If the equilibrium condition is met, print Φ , M and the obtained feature points:

6) When the limit damage point of the component is not calculated, $\varphi = \varphi + \delta\varphi$, turn 3), otherwise, the calculation ends.

(3) Axial force-moment interaction

Assume that the section bending moment is a function of the section curvature and the axial

force acting on the section, ie:

$$m = M(\phi, n)$$

Or incremental expression:

$$\Delta m = \frac{\partial M}{\partial \phi} \Delta \phi + \frac{\partial M}{\partial n} \Delta n = \left(\frac{\partial M}{\partial \phi} + \frac{\partial M}{\partial n} \frac{\Delta n}{\Delta \phi} \right) \Delta \phi$$

Compared to the typical beam equation, it can be seen that the section stiffness is:

$$(EI)_t = \frac{\partial M}{\partial \phi} + \frac{\partial M}{\partial n} \frac{\Delta n}{\Delta \phi}$$

(EI)_t is the section stiffness after considering the axial force change, Δn is the axial force increment, and $\Delta \Phi$ is the curvature increment. It can be seen from the formula that after considering the influence of the axial force, the current elastoplastic bending stiffness of the section

is composed of two parts, one of which $\frac{\partial M}{\partial \phi}$ is determined by the whole process curve of the bending moment-curvature of the section under the normal axial force. Tangent stiffness. The

second term $\frac{\partial M}{\partial n} \frac{\Delta n}{\Delta \phi}$ is that he represents the influence of the amount of change in the axial force

Δn . $\frac{\partial M}{\partial \phi}$ is obtained by finding the bending moment-axial force interaction curve of the section, which is the tangent slope of the bending moment-axial force action curve.

2.3. Structural Analysis Model

(1) Dynamic analysis of spatial structure

The motion differential equation of structural space vibration can be expressed as follows:

$$[M]\{\ddot{D}\} + [C]\{\dot{D}\} + [K][D] = -[M]\{\ddot{D}_g\}$$

Where: [M] is the mass matrix of the overall structure, [K] is the dynamic stiffness matrix of the overall structure; {D}, { \dot{D} }, { \ddot{D} } is the displacement and degree vector of the centroid of each rigid floor of the structure relative to the ground; { \ddot{D}_g } is the ground motion acceleration vector.

(2) Damping matrix

The Rayleighhg proportional damping is still used in the NLA.

$$[C] = \alpha_0[M] + \alpha_1[K]$$

$$\alpha_0 = 4\pi(\xi_1 T_1 - \xi_2 T_2) / (T_1^2 - T_2^2)$$

In the above formula: $\alpha_1 = T_1 T_2 (\xi_1 T_1 - \xi_2 T_2) / \pi (T_1^2 - T_2^2)$

T₁, T₂ is the first order, second order or third natural period of the structure.

ξ_1, ξ_2 is the damping ratio corresponding to the natural vibration period, and the default is 0.05 in the NLA.

[M] is the mass t matrix in the structural vibration differential equation. [K] uses the initial dynamic stiffness matrix [K₀].

(3) Solving the dynamic equation

The solution of the structural dynamic differential equation is based on the Wilson- θ method. The steps are:

1) Divide the entire seismic time history into a series of tiny time periods, each of which is called the step size and is recorded as Δt . Generally, equal steps are used. It is assumed that the stiffness matrix $[K]$ does not change within the step size Δt . Therefore, theoretically speaking, the smaller the Δt is, the higher the calculation accuracy is, but the calculation work t is also larger. $\Delta t=0.02s$ in NLA.

2) The actual seismic acceleration record or the artificially synthesized acceleration is recorded and quantified according to the time period Δt .

3) Treat $[C], [K], [\mathcal{E}_s]$ for each period as a constant value.

4) The increment value $\{\Delta D_i\}, \{\Delta \mathcal{E}_i\}, \{\Delta \mathcal{E}_i\}$ of the period is obtained by using the front end value $\{D_i\}, \{\mathcal{E}_i\}, \{\mathcal{E}_i\}$ of the $i+1$ th period (from the time t_i to the time t_{i+1}), and the end value $\{D_{i+1}\}, \{\mathcal{E}_{i+1}\}, \{\mathcal{E}_{i+1}\}$ is:

$$\begin{aligned}\{D_{i+1}\} &= \{D_i\} + \{\Delta D_i\} \\ \{\mathcal{E}_{i+1}\} &= \{\mathcal{E}_i\} + \{\Delta \mathcal{E}_i\} \\ \{\mathcal{E}_{i+1}\} &= \{\mathcal{E}_i\} + \{\Delta \mathcal{E}_i\}\end{aligned}$$

Step by step, step by step, to obtain the structural seismic response of the entire time course.

3. Experiment

3.1. Source of Data

Make three-layer, two-layer, two-span specimen test models, numbered KJ1, KJ2, KJ3-1, and KJ3-2. Among them, KJ1 is reinforced with C/GFRP hybrid fiber composite, KJ2 is reinforced with CFRP, KJ3-1 is used for comparison with reference frame, and FRP is not used for reinforcement. KJ3-2 is reinforced with CFRP after loading cracks in KJ3-1. To simulate the reinforcement of the test piece under use. KJ1 first pastes a layer of CFRP, and then pastes a layer of GFRP; KJ2 pastes two layers of CFRP. KJ3-2 is reinforced in the same way as KJ2. The reinforcement areas of the three-frame test piece model are nodes and columns.

For the FRP reinforcement of the frame edge node, the U-shaped wrapping and sticking method is mainly adopted, and the corner portion is chamfered and then FRP is used for bonding, so that the fiber is gently wound and closely attached to the column surface; for the node in the frame, a straight strip is adopted. The two sides of the fiber are covered and pasted respectively; the L-shaped anti-bending fiber strip is attached to the upper and lower sides of the beam and the column; for the end of the column, the overall hoop wrapping constraint is imposed, and the overlapping length of the fiber is not less than 150 mm.

3.2. Evaluation Criteria

Another problem that needs to be addressed in dynamic time history analysis is the seismic wave strength indicator. The ground motion of strong earthquakes has great complexity, and the damage ability of ground motion is mainly related to the amplitude, spectrum characteristics and strong earthquake holding time of ground vibration. The ground motion intensity index used in structural seismic analysis and research is the ground peak acceleration PGA.

According to the above research results, according to the provisions of China's "Code for Seismic Design of Buildings" (GB 50011-2010), "Design Rules for High-rise Concrete Structures"

(JGJ 3-2010) for structural elastoplastic time-history analysis, combined with the analysis of this paper. The example requires the selection of two US seismic records, the El Centro (NS) wave in May 1940, the Taft (S69E) wave in July 1952, and a set of artificial waves for seismic analysis. In this paper, based on the previous research results, combined with the recommendations of China's seismic code, the peak acceleration PGA of ground motion is used as the ground motion as the strength index.

4. Results

4.1. CAD Presentation and Dynamic Time History Analysis Comparison

In the dynamic time history analysis calculation, we know from experience that the maximum period of the building is usually $0.1 \cdot N$ seconds (N is the total number of floors of the building), and the minimum period is generally greater than 0.02 seconds. Therefore, we take the time step to 0.02 seconds to ensure the accuracy of the calculation, which means that the time step we selected is less than the minimum period value of the building. The Newmark- β method is basically reliable for all frequencies of the building and does not require the introduction of numerical damping. The amplitude of the high-frequency vibration is preserved, which is important because high-frequency vibration plays an important role in seismic analysis of some complex and irregular buildings. Therefore, in the dynamic time history analysis program SDY, we take $\gamma=0.5$. Table 1 lists the results of the elastic and elastoplastic time history analysis.

Table 1. Comparison of time-course analysis results

	Elastic analysis		Elastoplastic analysis			
	Top displacement	Time	Top displacement	Time	Base shear	Time
Frame a	51	13.08	280	3.72	31491	3.44
Frame b	48	3.72	311	3.74	27410	3.44
Frame c	46	14.62	263	3.74	15120	6.84
Frame d	43	14.58	240	3.70	27214	3.44
Frame e	51	3.74	333	3.76	23860	3.44

According to the analysis results in Table 1, we can see that in the case of elastic analysis, the seismic performance of frame (d) is optimal, while frame (a) is the worst. In the case of elastoplastic analysis, the seismic performance of frame (d) is optimal and frame (b) is the worst. Of course, the base shear force of the structure after the slanting bar is also increased a lot, and the base shear force in the case of the elastoplastic analysis listed in Table 1 illustrates this. From this we can also see that the frame (c) has the smallest base shear force in the case of large earthquakes, and the maximum displacement of the apex is not the largest in the frame with the diagonal bar. Moreover, although the frame with a slanted bar section of 300 mm x 600 mm has super-gluten phenomenon, this phenomenon does not occur in other frames with a slanted bar section of 300 mm x 700 mm. That is to say, according to the usual reasonable design, for the slanted rod structure under the condition of the present example, as long as the appropriate slanting rod section is selected, the requirement of "small exhibition is not bad" can be satisfied. In addition, it can be seen from the table that the slanted rod structure effectively limits the apex displacement and interlayer displacement of the structure, and the displacement angle between the elastoplastic layers is also within the allowable range of the specification, all satisfying the "big earthquake does not fall" Claim.

4.2. Time-history Analysis of Seismic Strengthening of Structures

Each frame skeleton curve is shown in Figure 1. It can be seen that the force-bearing processes of the four specimens are similar, from the elastic force stage to the yield stage, and then reach the maximum bearing capacity, and finally reach the limit state or damage; the bearing capacity and deformation capacity of the reinforcement frame are greatly improved. The ductility of the frame KJ1 (C/GFRP hybrid fiber reinforcement) is obviously improved, and the bearing capacity of the frame KJ2 (CFRP reinforcement) is obviously improved. The FRP-reinforced specimens exhibit good ductility and load-carrying capacity.

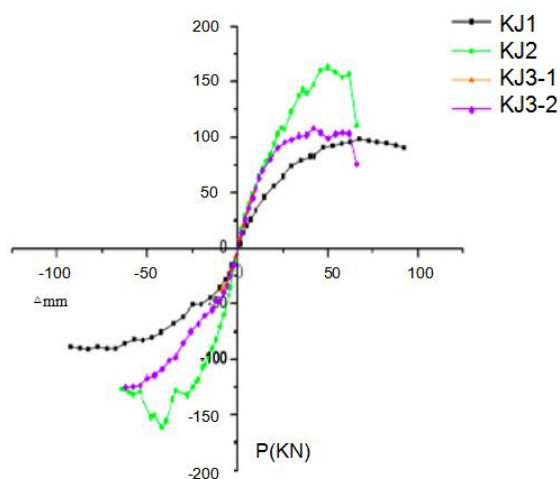


Figure 1. Skeleton curve of each frame

The frame skeleton curves of the frames KJ1, KJ2, and KJ3-2 are relatively full, but the pinching phenomenon is more obvious. In comparison, the bearing capacity of the frame KJ1 (CFRP reinforcement) is significantly higher than that of the frame KJ2 (C/GFRP hybrid fiber reinforcement), but the ductility is not as good as the frame KJ2. It shows that the FRP reinforcement bears part of the bending moment and shearing force of the joint zone and the end of the beam and column, which reduces the stress of the longitudinal reinforcement and delays the development of the crack, and improves the overall seismic performance of the frame. Among them, KJ2 has a large fluctuation in the peak value after yielding. The reason is that during the test, the steel pad of the column top hydraulic jack and the test piece is too thin, causing the shaft pressure loading point to sag, and the actuator needs to be larger during the loading process. The load can be reciprocally loaded, resulting in a large peak point.

According to the skeleton curve, the frame characteristic load and the characteristic displacement are determined as shown in Fig. 1. Wherein, the ultimate load takes the maximum load of the specimen during the loading process of the frame, and the ultimate displacement takes the displacement value of the frame to 85% of the ultimate bearing capacity. If the frame fails to reach 85% of the ultimate bearing capacity, then Take the maximum displacement value of the previous cycle.

4.3. Elasto-plastic Dynamic Time History Analysis of Materials

The seismic strengthening effects of C/GFRP and CFRP fiber materials were compared respectively, and three different schemes were analyzed and compared: reinforcing the first layer, reinforcing the first layer to the third layer, and reinforcing the reinforcement layer. Under the

action of El seismic wave and Taft wave, the maximum interlayer displacement angle of C/GFRP, CFRP reinforced and unreinforced frame structures is used, as shown in Fig. 2.

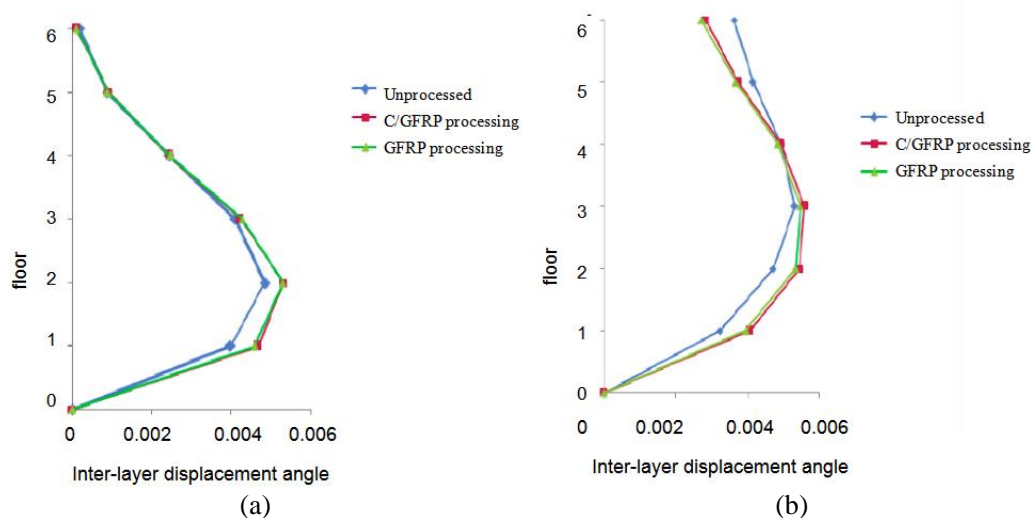


Figure 2. El-Centro seismic wave (a) Inter-layer displacement angle under Taft seismic wave (b)

The reinforcement frame has a certain degree of improvement compared with the unreinforced structure, and the effect of C/GFRP reinforcement is slightly better than that of CFRP reinforcement, but it is not obvious, indicating that the reinforcement of the reinforced concrete frame joints with FRP can effectively improve the structure. Ductility. The maximum interlayer displacement angle of the C/GFRP-reinforced frame is used in three different schemes, as shown in Figure 2(b). Both scheme 1 and scheme 2 have improved the ductility of the framework, but under the action of Taft waves, the phenomenon of weak layer transfer has occurred. In combination with Figure 2, the use of two FRP materials using Scheme 1 and Scheme 2 reinforcement results in a weak layer transfer in the structure. The reinforcement method of scheme 3 does not show the transfer of weak layers, and the displacement angle between layers is reduced relative to the unreinforced frame. This is due to the reinforcement of the nodes of all layers, and the reason for the structural rigidity to be improved to some extent. The lateral displacement capability of the structure.

5. Discussions

From the analysis results in Table 1, we also found that in the case of elastic analysis, the maximum displacement of the apex of the frame with the diagonal bar (a) is as large as the maximum displacement of the unslanted bar, and we have already found that the slanting bar is significant. The conclusion that the seismic performance of the frame structure is enhanced. This is because when the structure reaches a certain number of layers, when the grounding force suffered by the structure reaches a certain level, the effect of the diagonal rod becomes very limited, and sometimes it will have a negative effect - the inclined rod itself increases the self-weight of the structure, resulting in an increase in the seismic force of the structure.

The yield loads of KJ2 and KJ3-2 are both greater than KJ1. It can be seen that the CFRP reinforcement frame has better yield load than C/GFRP hybrid fiber. However, hybrid fibers participate in work earlier than carbon fibers. The ultimate bearing capacity of KJ2 is 131k N, followed by KJ3-2, which is 125.5k N, and the ultimate bearing capacity of KJ1 is 98.9k N. CFRP reinforcement is better than C/GFRP hybrid fiber in improving the overall load carrying capacity of the frame.

Both C/GFRP reinforcement and CFRP reinforcement can improve the seismic performance of

reinforced concrete frames. C/GFRP is slightly better than CFRP in improving ductility. CFRP reinforcement is better in earthquake resistance, but it is not obvious. Considering that the GFRP reinforcement effect is similar to that of CFRP, the lower price of GFRP material can reduce the reinforcement cost; the three reinforcement schemes can improve the ductility of the concrete frame structure, but adopt scheme 1 (only reinforcement layer 1) and scheme 2 (Reinforcement of Tier 1 to Tier 3) may result in the transfer of weak layers.

6. Conclusion

In this paper, the dynamic time history analysis of building structure CAD is carried out by comparing the dynamic time history analysis, the seismic strengthening of the structure and the elastoplasticity of the material, and the following conclusions are obtained:

(1) When selecting the appropriate cross section of the inclined rod, it can meet the requirement of “small earthquake is not bad”: at the same time, it can eliminate the weak layer, effectively limit the apex displacement and interlayer displacement of the structure, and control the displacement angle between the elastoplastic layers. Within the scope of the specification, it meets the requirements of “the big earthquake does not fall”. Under horizontal static loading, reinforced concrete split-frame structures are more effective in limiting lateral displacement than pure frame structures.

(2) The dynamic elastoplastic time-history analysis method can accurately reflect the three elements of ground motion: peak, spectrum and time-keeping, and then accurately and comprehensively analyze the structure from the internal forces, deformations and structural members of the linear and nonlinear phase structures in the earthquake. The whole process of cracking, yielding and breaking to the final collapse; the dynamic elastoplastic time history analysis of reinforced concrete strengthened by FRP seismic analysis shows that the FRP-based joint-based seismic strengthening reinforced concrete frame can effectively improve its bearing capacity, ductility and energy dissipation capacity. Such as seismic performance.

(3) C/GFRP reinforcement and CFRP reinforcement can improve the seismic performance of reinforced concrete frame. C/GFRP is slightly better than CFRP in improving ductility. CFRP reinforcement effect is better in earthquake resistance, but it is not obvious. Considering that the GFRP reinforcement effect is similar to that of CFRP, but the price of GFRP material is lower, it is recommended to consider the reinforcement cost; the three reinforcement schemes can improve the ductility of the concrete frame structure, but adopt the first scheme (only reinforcement of the first layer) and Option 2 (reinforcement of Tier 1 to Tier 3) may result in the transfer of weak layers.

Funding

This article is not supported by any foundation.

Data Availability

Data sharing is not applicable to this article as no new data were created or analysed in this study.

Conflict of Interest

The author states that this article has no conflict of interest.

References

- [1] Vikram A, Agarwal V, Agarwal A. *Lithography technology for advanced devices and introduction to integrated CAD analysis for hotspot detection*. *IET Circuits, Devices & Systems*, 2017, 11(1):1-9. DOI: 10.1049/iet-cds.2015.0325
- [2] Yu R, Fang Q, Chen L, et al. *Performance-based blast-resistant design of building structure components*. *Gong Cheng Li Xue/Engineering Mechanics*, 2016, 33(11): 75-83.
- [3] Brouwer D H, Cadars S, Hotke K, et al. *Structure determination of a partially ordered layered silicate material with an NMR crystallography approach*. *Acta Crystallographica Section C Structural Chemistry*, 2017, 73(3): 184-190. DOI: 10.1107/S2053229616019550
- [4] Hartmann Andr e Gotthard M, Robert H, et al. *A Workflow for Automatic Quantification of Structure and Dynamic of the German Building Stock Using Official Spatial Data*. *ISPRS International Journal of Geo-Information*, 2016, 5(8):142. DOI: 10.3390/ijgi5080142
- [5] Russo D. *A Computer Aided Strategy for More Sustainable Products*. *Ifip Advances in Information & Communication Technology*, 2017, 355:149-162.
- [6] Wei G, Dong K, Liu Q, et al. *Facile preparation of a silica-sphere-poly(catechol hexamethylenediamine) composite for the competitive removal of cadmium(II), lead(II), and copper(II) ions*. *Journal of Applied Polymer Science*, 2018, 135(8): 45839.
- [7] Li L, Tang H, Guo S, et al. *Design and implementation of an integral design CAD system for plastic profile extrusion die*. *International Journal of Advanced Manufacturing Technology*, 2016, 89(1-4): 1-17. DOI: 10.1007/s00170-016-9099-x
- [8] Li Xiaoxu. *Discussion on the application of CAD drawing software in four fields of clothing, architecture, machinery and electronics*. *China Off-campus Education*, 2017(25):65+71.
- [9] Ren Zhenyu. *Application of CAD Technology in Structural Design of High-rise Buildings*. *Automation & Instrumentation*, 2017(10):161-162+165.
- [10] Yan Shuaiping, Zhang Yinfang. *Analysis of seismic design in structural design of building engineering*. *Green building materials*, 2019(05):81+83.
- [11] Yao Xianchun, Yao Wei, Zhang Wei, Yao Jun, Xie Haixiang. *Directive Blasting Demolition of High-rise Frame-Shear Structure*. *Explosive Materials*, 2019(03):49-54.
- [12] Liu S W, Bai R, Chan S L. *Dynamic Time-history Elastic Analysis of Steel Frames Using One Element per Member*. *Structures*, 2016, 8:300-309.
- [13] Samuel B, Rethesh R, Ansari MZ, et al. *Cross-correlation and time history analysis of laser dynamic specklegram imaging for quality evaluation and assessment of certain seasonal fruits and vegetables*. *Laser Physics*, 2017, 27(10):105601.
- [14] Choine M N, Kashani M M, Lowes L N, et al. *Nonlinear dynamic analysis and seismic fragility assessment of a corrosion damaged integral bridge*. *International Journal of Structural Integrity*, 2016, 7(2): 227-239.
- [15] Tong Z, Hongshuai L, Xiaoming Y, et al. *Time history response analysis of landslide mass reinforced by Anchorage pile based on dynamic centrifugal test*. *Journal of Natural Disasters*, 2017, 26(3): 39-47.
- [16] Li S, Zuo Z, Zhai C, et al. *Comparison of static pushover and dynamic analyses using RC building shaking table experiment*. *Engineering Structures*, 2017, 136:430-440.
- [17] Koo R C H, Kwan J S H, Sze E H Y. *Stability assessment of soil slopes subject to blasting vibrations based on time history analyses*. *HKIE Transactions*, 2016, 23(3): 130-137.